DOI: 10.1002/ejic.201000968

Ruthenium–Porphyrin Complexes Induce Apoptosis by Inhibiting the Generation of Intracellular Reactive Oxygen Species in the Human Hepatoma Cell Line ($HepG_2$)

Yanan Liu,[a,b] Xiaonian Zhang,[a] Rong Zhang,[a] Tianfeng Chen,[a] Yum-Shing Wong,[b] Jie Liu,*[a] and Wen-Jie Zheng*[a]

Keywords: Ruthenium / Antitumor agents / Apoptosis / Antioxidants / Radical scavengers

Two ruthenium(II)–porphyrin complexes, [(3-Py)Ru(phen)$_2$(tmopp)] [**1**; phen = phenanthroline, tmopp = 5,10,15,20-tetrakis(4-methoxyphenyl)porphyrin] and [(4-Py)Ru(phen)$_2$(tmopp)] (**2**), have been synthesized and characterized for the first time. It was found that the two ruthenium(II)–porphyrin complexes show significant antitumor activity in $HepG_2$ cells. Flow cytometric analysis showed that complex **1** arrested the cell cycle in the G0/G1 phase and induced apoptosis in $HepG_2$ cells. Fluorescence microscopy and flow cytometric analyses demonstrated that the generation of intracellular reactive oxygen species (ROS) was significantly inhibited in cells treated with either complex. The total antioxidant capacity of the complexes was detected by a 2,2′-azinobis(3-ethylbenzthiazoline-6-sulfonic acid) (ABTS) assay; this showed that both complexes are good free-radical scavengers. Ruthenium(II)–porphyrin complex **1** also was found to scavenge hydroxy radicals, as measured by the Fenton system. These data demonstrate that ruthenium(II)–porphyrin complexes exhibit antioxidant properties, probably through the involvement of a direct scavenging effect on a hydroxy radical. Taken together, the findings show that ruthenium(II)–porphyrin complexes induce apoptosis in $HepG_2$ cells by inhibiting the generation of ROS and are potential anticancer therapeutic agents.

Introduction

Since cisplatin was developed as an anticancer drug, the synthesis and antitumor activity of inorganic metal complexes have received widespread attention. The purpose is to find drugs that have lower toxicity but more activity than cisplatin.[1–3] Investigations into new anticancer drugs have highlighted ruthenium as a potential metal center for new therapies.[4–6] Ruthenium possesses several favorable properties: it exhibits cytotoxicity against cancer cells, has similar ligand-exchange abilities as platinum complexes, has no cross-resistance with cisplatin, is easily absorbed and rapidly excreted by the body, and may have reduced toxicity against healthy tissues due to transferrin transport.[7–11] Ru complexes have previously been shown to be among the most promising anticancer drugs.[12,13] A number of Ru complexes have displayed promising anticancer activity.[14,15] Porphyrins and their derivatives are widely used in modern medicine as contrast agents for cancer diagnostics and as sensitizers in photodynamic therapy due to their spectral characteristics, phototoxicity, and high affinity for tumor tissues. Porphyrins play a significant role in the diagnosis and treatment of cancer.[16] Over the last decade, ruthenium–porphyrin complexes have attracted much attention due to their potential application as anticancer drugs.[17] However, the molecular mechanisms of the apoptosis-inducing action of ruthenium porphyrin complexes remain to be elucidated.

In recent years, numerous studies showed that free radicals, especially reactive oxygen species (ROS), are important in the regulation of apoptosis.[18] Changes in the level of ROS that precede morphological changes have been shown to be an important way to induce apoptosis.[19] A great number of studies have reported that, in the process of cell apoptosis, ROS can also participate in cell-signal transduction, start the expression of some genes of apoptosis, and have complicated correlations with a variety of biological molecules, including those that belong to the B-cell lymphoma 2 (bcl-2) family, caspases, and mitochondrial permeability transition (PT) pore complex.[20] Many ruthenium complexes have been reported that exhibit both antioxidant activity and antitumor activity.[21] Therefore, studies on the relationship between the antitumor activity of drugs and the level of ROS have vital significance.

At present, studies on the mechanisms of action of ruthenium complexes have been mainly focused on its targets, such as DNA and protein, whereas its antioxidant activity has been rarely reported.[22] Our current investigations in this paper attempt to elucidate the molecular mechanism

[a] Department of Chemistry, Jinan University, Guangzhou 510632, China
Fax: +86-20-8522-1263
E-mail: tliuliu@jnu.edu.cn
[b] Department of Biology, The Chinese University of Hong Kong, Hong Kong, China

Supporting information for this article is available on the WWW under http://dx.doi.org/10.1002/ejic.201000968.

that underlies such activity by ruthenium–porphyrin complexes. We have examined the relationship between the antitumor and antioxidant properties of ruthenium complexes in the $HepG_2$ tumor model. In addition, we assessed the scavenging capability of free radicals of the two ruthenium complexes by using in vitro molecular techniques. Ruthenium–porphyrin complexes exhibit antioxidant activity and might be responsible for complex-induced apoptosis.

Results and Discussion

Synthesis and Characterization

The ruthenium–porphyrin complexes were readily synthesized in excellent purity by following the procedures reported in the Exp. Section. Complexes **1** and **2** were characterized by elemental analyses, UV/Vis spectroscopy, and ESI-MS. The bonding arrangement was further confirmed by ^1H NMR spectra. The molecular structures of the ruthenium–porphyrin complexes are shown in Scheme 1.

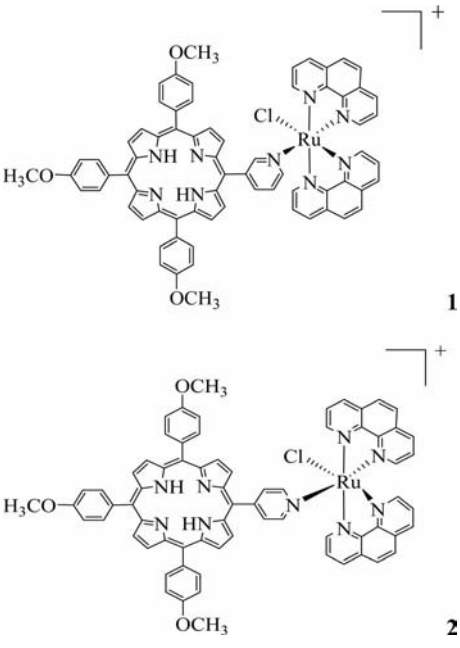

Scheme 1. [(3-Py)Ru(phen)$_2$(tmopp)] (**1**) and [(4-Py)Ru(phen)$_2$(tmopp)] (**2**) [phen = phenanthroline; tmopp = 5,10,15,20-tetrakis(4-methoxyphenyl)porphyrin].

Blocking the Growth of $HepG_2$ Cells

Cell death is characterized by obvious morphological characteristics. $HepG_2$ cells treated by ruthenium complexes with different concentrations showed clear morphological change and quantity decrease, as shown in Figure 1. The morphological change of the cells is positively correlated with dosage, and significant apoptotic bodies were observed with higher complex concentration. These phenomena suggest that ruthenium–porphyrin complexes block the growth of $HepG_2$ cells.

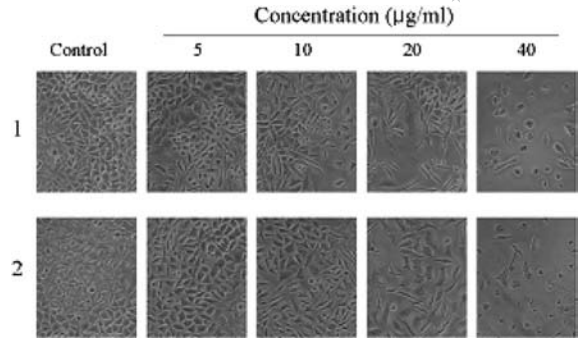

Figure 1. Morphology of $HepG_2$ cells upon incubation with 5, 10, 20, and 40 μM complexes **1** and **2**.

To further observe and study the antitumor activity of these ruthenium–porphyrin complexes, cell viability was determined by a 3-(4,5-dimethylthiazol-2-yl)-2,5-diphenyltetrazolium bromide (MTT) assay. As displayed in Figure 2, increasing complex concentrations decrease the $HepG_2$ cell viability in a dose-dependent manner. Furthermore, complex **1** appears to be more effective in inhibiting $HepG_2$ cell growth.

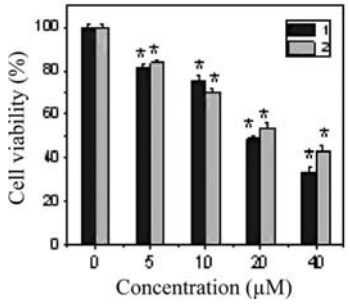

Figure 2. Cell viability after treatment with different concentrations of the complexes for 48 h as examined by the MTT assay. The significance of the differences between the mean values were determined by using a student's t test. Results were considered significant at $p < 0.05$, which are marked by *.

The IC_{50} values, calculated from the dose-survival curves obtained after 48 h of drug treatment with the MTT assay, are shown in Table 1. The IC_{50} values for complex **1** and **2** are (18.7 ± 1.3) and (23.6 ± 3.9) $\mu g\,mL^{-1}$, respectively, thus confirming that complex **1** is more active than complex **2** toward $HepG_2$ cells.

Table 1. Growth inhibition of ruthenium–porphyrin complexes on $HepG_2$ cells.[a]

Complex	**1**	**2**
IC_{50} [$\mu g\,mL^{-1}$]	18.7 ± 1.3	23.6 ± 3.9

[a] Cells were treated with various concentrations of tested complexes for 48 h.

G0/G1-Phase Arrest and Apoptosis of HepG2 Cells

In general, inhibition of cancer-cell proliferation by cytotoxic drugs could be the result of induction of apoptosis or

of cell cycle arrest, or a combination of these two modes.[20,23] According to the results of the MTT assay (Table 1), complex **1** is more active than complex **2** in inhibiting $HepG_2$ cell growth. Thus, this complex was used for further investigation of the underlying mechanisms. Flow cytometric analysis was carried out to determine the possible mechanisms of cell-growth inhibition. Figure 3 shows the representative DNA distribution histograms of $HepG_2$ cells incubated in the absence or presence of 10 and 20 $\mu g\,mL^{-1}$ complex **1** for 72 h. Exposure of $HepG_2$ cells to complex **1** led to a marked dose-dependent increase in the proportion of apoptotic cells, as reflected by the subdiploid peaks. Moreover, treatment with complex **1** caused a dose-dependent increase in the percentage of cells at the G0/G1 phase, accompanied by a corresponding reduction in the percentage of cells at G2/M phase and S phase, thereby indicating the induction of G0/G1-phase arrest by complex **1**.

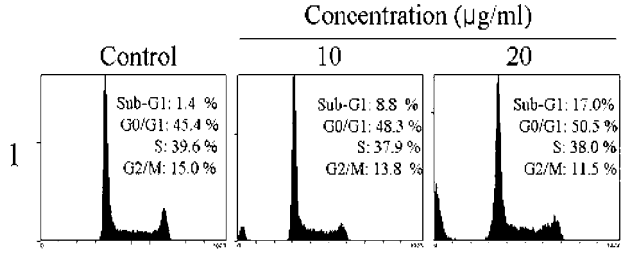

Figure 3. Effects of complex **1** on apoptosis and cell-cycle distribution in $HepG_2$ cells. The cells were treated for 72 h, collected, and stained with propidium iodide after fixation as described in the Exp. Section. These values were from a representative result of three independent experiments.

Intracellular ROS Levels

ROS, as signal molecules and effector molecules in apoptosis, have been shown to play an important role in apoptosis induced by a variety of factors. We next investigated whether the cell death induced by ruthenium–porphyrin complexes is dependent on ROS levels.

We treated $HepG_2$ cells with complex **1** and measured their level of intracellular ROS by using 2′,7′-dichlorofluorescin (DCF) fluorescence. This assay is based on the cellular uptake of a nonfluorescent probe, 2′,7′-dichlorofluorescein diacetate (DCFH-DA), which is subsequently hydrolyzed by intracellular esterase to form dichlorofluorescein (DCFH). The nonfluorescent substrate is oxidized by intracellular free radicals to produce a fluorescent product DCF. The level of ROS production is linearly proportional to the fluorescence intensity of DCF.[24] As shown in Figure 4, ROS generation in $HepG_2$ cells treated with complex **1** decreased with increasing complex concentration as indicated by decreasing DCF intensity. Therefore, ruthenium–porphyrin complexes reduced the level of intracellular ROS.

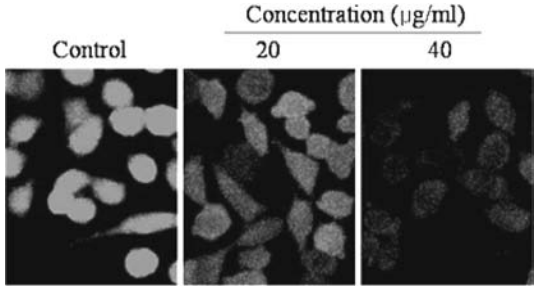

Figure 4. DCF fluorescence images of $HepG_2$ cells treated with complex **1**. Cells were treated with various concentrations of tested complex for 30 min.

We obtained similar results with a DCFH-DA flow cytometric assay (Figure 5). When cells were exposed to different concentrations of complex **1** or **2** for 15, 30, and 60 min, we observed a marked dose-dependent decrease in the level of intracellular ROS. The results showed that both complexes inhibit the level of ROS generation to different extents, thereby suggesting that ruthenium complexes may have antioxidant activity in vivo.

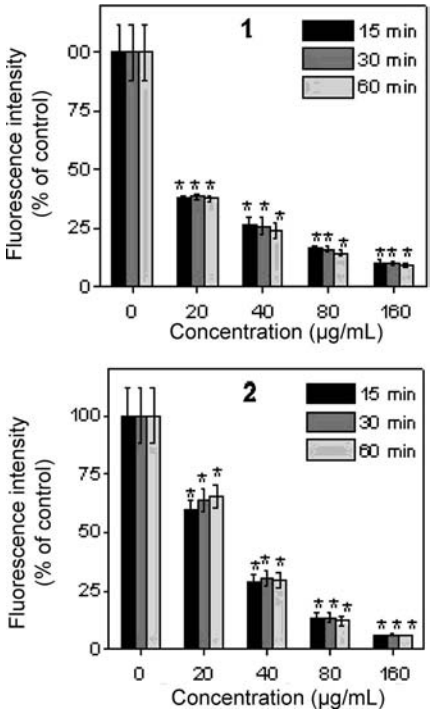

Figure 5. Intracellular ROS generation in $HepG_2$ cells treated with complexes **1** and **2**. Cells were treated with different concentrations of the complexes for 15, 30, and 60 min. The significance of the differences between the mean values were determined by using a student's *t* test. Results were considered significant at $p < 0.05$, which are marked by *.

Clean Up of the Oxygen Free Radicals in In Vitro Tests

The 2,2′-azinobis(3-ethylbenzthiazoline-6-sulfonic acid) (ABTS) radical cation decolorization assay, established by Miller in 1996,[25] has been widely used to determine the total antioxidant capacity of biological samples. We used this assay to study the radical scavenging activity of the ruthenium–porphyrin complexes. This method is based on the ability of antioxidant molecules to quench the stable radical cation $ABTS^{\cdot+}$, a blue-green chromophor with char-

acteristic absorption at 734 nm. In this system, greater bleaching of the solution indicates stronger total antioxidant capacity of the detected material.

Determining the Wavelength of the ABTS Reaction System

In this study, the UV/Vis absorption spectra of ABTS and ruthenium–porphyrin complexes were measured, respectively. The results show that the radical cation ($ABTS^{\cdot+}$) has a characteristic absorption spectrum with maxima at 415 and 734 nm, and the ruthenium–porphyrin complex has a strong absorption peak in the 400–500 nm range but no absorption peak at 734 nm. Therefore, to prevent interference caused by the absorption peaks of the ruthenium–porphyrin complex, we used 734 nm as the detection wavelength for the ABTS free-radical scavenging assay.

UV/Vis Absorption Spectrum Titration Experiments

The UV/Vis absorption spectrum was determined upon addition of complex **1** and **2** to the ABTS radical solution. We observed dose-dependent decreases in the absorption peak at 734 nm (Figure 6), thereby suggesting that both ruthenium–porphyrin complexes can clear ABTS free radicals. This can explain why ruthenium–porphyrin complexes have antioxidant activity. Again, there is evidence that complex **1** has a stronger free-radical scavenging ability, and hence stronger antioxidant activity because the ABTS absorption peak of complex **1** was reduced more significantly when used at the same concentration as for complex **2**.

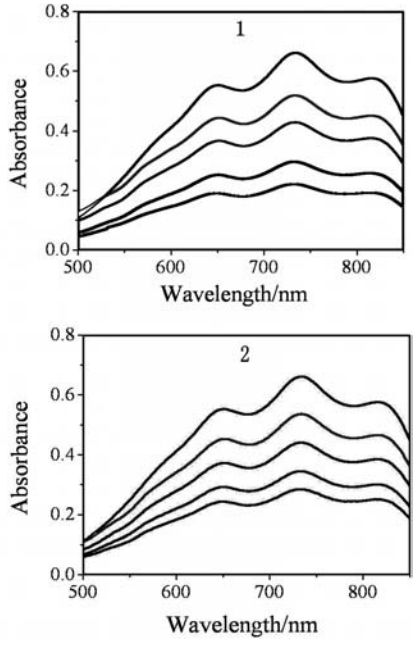

Figure 6. Changes in absorbance spectra of ABTS with addition of complexes **1** and **2**.

The Reaction Kinetics of the ABTS System

In the ABTS free-radical scavenging experiment, the response time of the reaction system is a key influencing factor for different antioxidants.[25] To understand the characteristics of the ABTS system reaction kinetics used in this experiment, different concentrations of ruthenium–porphyrin complexes were added to the ABTS radical solution and the absorbance was detected with equal time intervals. The results are shown in Figure 7. We observed that, after adding the two complexes (100–1600 μM) to the ABTS radical solution, both complexes produced a significant decrease of characteristic absorption peak at 734 nm. However, the characteristic absorption peak at 734 nm of complex **1** was reduced to a greater extent than that of complex **2** under the same concentration and time conditions. Therefore, complex **1** shows stronger free-radical scavenging ability and antioxidant activity.

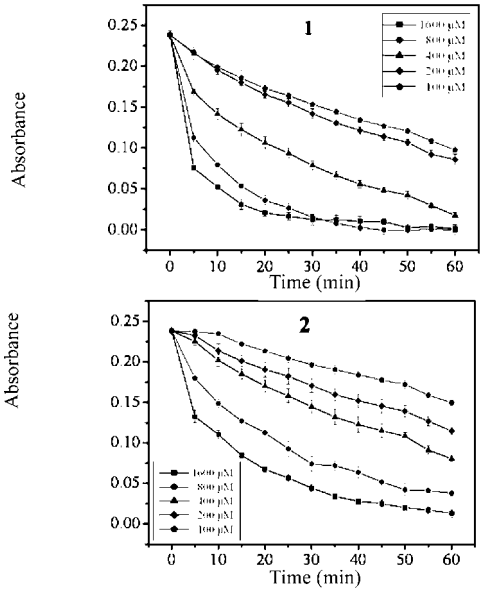

Figure 7. Changes in absorbance of ABTS after adding different concentrations of complexes **1** and **2** for different times.

Effect of Ruthenium Complex 1 on Hydroxy Radicals

Hydroxy radicals ($OH^{\cdot}$) were generated in a Fenton-type system. The ability of ruthenium complex **1** to scavenge this free radical was tested. Figure 8 depicts the inhibitory effect

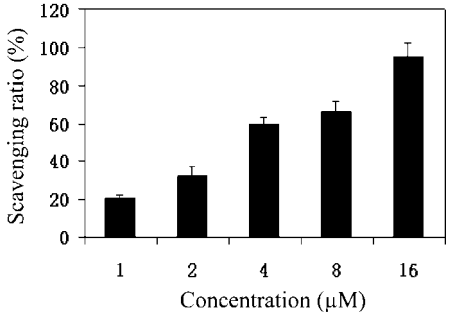

Figure 8. Scavenging effect of complex **1** on hydroxy radicals. Experiments were performed in triplicate.

of ruthenium complex **1** on $OH^{\cdot}$; the average suppression ratios for $OH^{\cdot}$ increase with the increasing concentration of ruthenium complex **1** in the range of 1–16 μM. The suppression ratio against $OH^{\cdot}$ ranged from 20.69 to 95.40%. Due to the lower IC_{50} (3.04 μM) value, ruthenium complex **1** may be a potential free-radical scavenger.

Conclusion

The complexes [(3-Py)Ru(phen)$_2$(tmopp)] (**1**) and [(4-Py)Ru(phen)$_2$(tmopp)] (**2**) were synthesized and characterized. In vitro experiments show that both complexes have growth-inhibitory effects on $HepG_2$ cells, with complex **1** being more highly effective at inducing G0/G1 cell-cycle arrest and apoptotic cell death in $HepG_2$ cells. The level of intracellular ROS decreased significantly after the treatment with both complexes. An ABTS assay revealed that both complexes are able to scavenge free oxygen radicals. Complex **1** was also found to be able to scavenge hydroxy radicals. From these data we conclude that ruthenium–porphyrin complexes may have antioxidant activity. One possible and important mechanism is the reduction of the level of intracellular ROS by scavenging hydroxy radicals, and thus inducing $HepG_2$ cell apoptosis.

Experimental Section

General Conditions: $RuCl_3{\cdot}nH_2O$ (AR) was obtained from the Kunming Institute of Precious Metals. Tris(hydroxymethyl)aminomethane (Tris) and 2,2′-azinobis-3-ethylbenzothiazolin-6-sulfonic acid (ABTS) were purchased from the Sigma Company. Tris/HCl buffer (50 mM, pH = 7.4) was prepared by physiological saline. Stock solutions (0.4 mM) of the ruthenium–porphyrin complexes were prepared in the appropriate culture medium with 10% fetal bovine serum and diluted by culture medium to various working concentrations, which were obtained by serial dilutions. All other chemicals and solvents were reagent grade, purchased commercially and used without further purification unless stated otherwise.

Cell Culture: The $HepG_2$ human hepatoma cell line was obtained from the American Type Culture Collection (ATCC, Manassas, VA) and was cultured in RPMI 1640 medium that contained 10% fetal bovine serum, 100 units mL^{-1} penicillin, and 50 units mL^{-1} streptomycin at 37 °C in a humidified incubator under 5% CO_2 atmosphere. Cells from a confluent monolayer were removed from flasks by 0.25% trypsin/ethylenediaminetetraacetic acid (EDTA) solution. Cell viability was determined by the trypan blue dye exclusion test.

Synthesis and Characterization

(3-Py)tmopp: (3-Py)tmopp was synthesized according to the literature[26] Briefly: A mixed solution that contained propionic acid (30 mL), 3-pyridinecarbaldehyde (0.019 mol), and pyrrole (0.075 mol) was added dropwise into propionic acid solution (120 mL) that contained *p*-methoxybenzaldehyde (0.056 mol) with stirring and was heated to reflux at 120 °C for 40 min. The cooled, mixed solution was diluted with ethanol (100 mL) and frozen for 24 h. The mixture was filtered and the purple precipitates were washed with ethanol several times and then dried. The crude product dissolved in chloroform was purified by filtration through silica gel (60–100 mesh). The second purple band was collected. Then, by evaporation of the solution, purple powder was obtained, and it was dried in vacuo; yield 0.722 g (5.3%).

(4-Py)tmopp: This ligand was synthesized in an identical manner to that described for (3-Py)TMOPP with 4-pyridinecarbaldehyde in place of 3-pyridinecarbaldehyde; yield 0.871 g (6.4%).

cis-[Ru(phen)$_2$Cl$_2$]·2H$_2$O: [Ru(phen)$_2$Cl$_2$]·2H$_2$O was prepared following the literature and was determined to be the identical compound.[27] A mixture of $RuCl_3{\cdot}nH_2O$ (6 mmol), phenanthroline (12 mmol), and lithium chloride (28 mmol) in DMF (10 mL) was heated to reflux under argon for 8 h. The cooled, mixed solution was diluted with acetone (50 mL) and frozen for 24 h. The mixture was filtered. The precipitates were washed with ice water and acetone several times and dried in vacuo. A purple-black microcrystalline was obtained; yield 1.66 g (49%) (calculated from phenanthroline).

[(3-Py)Ru(phen)$_2$(tmopp)] (1): A mixture of (3-Py)tmopp (0.36 mmol) and *cis*-[Ru(phen)$_2$Cl$_2$]·2H$_2$O (0.3 mmol) in acetic acid (20 mL) was heated to reflux under argon for 3 h. Then, by evaporation of the solution, the crude product was obtained. The crude product was dissolved in chloroform and purified by filtration through silica gel (60–100 mesh) with chloroform and methanol (2:1 v/v) as eluant. The band that was predominantly purple was collected. The solvent was removed under reduced pressure and a purple-black powder was obtained; yield 0.086 g (20.9%). Elemental analyses were performed with a Perkin–Elmer LS55 Elemental Analyzer. ^{1}H NMR: δ = 8.83 (d, 2 H), 8.73 (d, 2 H), 8.61 (d, 4 H), 8.32 (s, 4 H), 8.15 (d, 2 H), 7.88–7.94 (m, 2 H), 7.52 (d, 2 H), 7.21–7.34 (m, 12 H), 7.12 (d, 2 H), 4.02 (d, 8 H), 3.31 (s, 9 H) ppm. $[C_{70}H_{51}N_9O_3ClRu]Cl$ (1202.28): calcd. C 69.90, H 4.27, N 10.48; found C 70.03, H 4.42, N 10.73. UV/Vis (CH_3CN): λ (10^{-4} ε, M^{-1}cm^{-1}) = 654.0 (0.2), 594.0 (0.5), 560.5 (0.9), 523.0 (1.4), 410.5 (12.4) and 267.5 (2.6) nm. ESI-MS: *m*/*z*: 1202 $[M]^+$.

[(4-Py)Ru(phen)$_2$(tmopp)] (2): This complex was synthesized in an identical manner to that described for **1** with (4-Py)tmopp in place of (3-Py)tmopp; yield 0.065 g (14.2%). ^{1}H NMR: δ = 8.88–8.73 (d, 6 H), 8.58 (d, 2 H), 8.31 (s, 4 H), 8.19 (d, 2 H), 8.05 (d, 6 H), 7.71–7.83 (m, 2 H), 7.52–7.75 (m, 10 H), 7.48 (d, 2 H), 7.24 (d, 2 H), 7.15 (d, 2 H), 3.35 (s, 9 H) ppm. $[C_{70}H_{51}N_9O_3ClRu]Cl$ (1202.28): calcd. C 69.90, H 4.27, N 10.48; found C 70.11, H 4.59, N 11.00. UV/Vis (CH_3CN): λ (10^{-4} ε, M^{-1}cm^{-1})=656.0 (0.3), 598.0 (0.6), 567.0 (1.0), 523.5 (1.3), 432.5 (14.6) and 268.5 (3.5) nm. ESI-MS: *m*/*z*: 1202 $[M]^+$.

Cell Viability Assay: The cytotoxicity of ruthenium–porphyrin complexes was determined by the MTT assay, a colorimetric assay based on the ability of the viable cells to reduce a soluble yellow tetrazolium salt to blue formazan crystals.[28,29] Cells were removed from flasks by trypsin solution and their viability determined by the trypan blue exclusion test. They were seeded into 96-well plates at a density of 2×10^4 cells per mL and left to grow overnight. The cells were treated by adding a solution (100 μl) that contained the test complexes, with each reaction in triplicate. In each instance, cells were left to grow for 48 h before treatment with MTT (20 μl, 5 mg mL^{-1}) reagent for 5 h (Sigma, St. Louis, MO). After this time, the medium was aspirated and replaced with DMSO (150 μl) per well to dissolve the formazan salt. The color intensity of the formazan solution, which reflects the cell-growth conditions, was measured at 570 nm with an ELX800 type Microplate Reader (Bio-Tek, USA). The percentages of surviving cells relative to untreated controls were determined. The IC_{50} values, defined as the drug con-

centration that inhibits cell growth by 50%, were estimated from semilogarithmic dose–response plots.[30]

Cell-Cycle Analysis and Apoptosis Assays: Flow cytometric analysis was carried out according to our previous method. Briefly, one million cells, as determined by trypan blue exclusion test, were washed in cold phosphate buffer solution (PBS) and fixed in 70% ethanol at –20 °C overnight. The fixed cells were washed twice with PBS, re-suspended in PBS (1 mL) that contained RNase A (0.25 mg), EDTA (2 mM), and propidium iodide (0.1 mg). This was incubated at 37 °C for 30 min, and cells were analyzed. The fluorescence of 10000 cells was measured with a Beckman Coulter Epics XL-MCL flow cytometer (Miami, FL). The cell-cycle distribution was analyzed by MultiCycle software (Phoenix Flow Systems, San Diego, CA). The proportions of cells in the G0/G1, S, and G2/M phases were represented as DNA histograms. Apoptotic cells were measured by quantifying the sub-G_1 peak.

Measurement of Intracellular ROS: The effects of ruthenium–porphyrin complexes on the generation of intracellular ROS were evaluated by the DCF fluorescence assay. Briefly, cells were harvested by centrifugation, washed twice with PBS, and suspended in PBS (1×10^6 cells mL^{-1}) with DCFH-DA (10 mM) at 37 °C for 50 min. The cells were washed three times with Hank's solution to remove extracellular fluorescent agent and suspended in Hank's solution (500 μL). After the addition of complexes, cells were incubated at 37 °C for different lengths of time and analyzed by flow cytometry.

ABTS Assay: The scavenging capability of free radicals of the two ruthenium complexes was determined by using the $ABTS^{\cdot+}$ method described by Hempel et al.[31] The ABTS stock solution (5 mM) was prepared with PBS (pH = 7.4), and the ABTS cation radical ($ABTS^{\cdot+}$) was produced by reaction of ABTS cation (5 mM) with manganese dioxide in water and filtered with polyvinylidine fluoride (PVDF) membrane (0.2 μm) after the reaction. This was diluted with PBS (pH = 7.4) to an absorbance of 0.70 ± 0.02 at 734 nm and stored at –20 °C. The experimental procedure was as follows: Different concentrations of sample or reference solution (DMSO; 50 μL) were added to a 10 mL colorimetric tube, immediately followed by the addition of ABTS reaction solution (3 mL). The reaction mixture was shaken and the mixture was allowed to stand in the darkness at room temperature for 6 min. Absorbance was measured by Lambda-850 UV/Vis spectroscopy (Perkin–Elmer, USA) at 734 nm. The percentage of inhibition of $ABTS^{\cdot+}$ (I%) was calculated from Equation (1).

$$I(\%) = (1 - A_S/A_0) \times 100\% \quad (1)$$

In this equation, A_S is the absorbance of the sample tube, and A_0 is the absorbance of the control tube.

Hydroxy Radical-Scavenging Activity: The hydroxy radical ($OH^{\cdot}$) in aqueous media was generated by the Fenton system.[32] The solution of the tested complexes was prepared with DMSO, safranin (20 μg mL^{-1}), EDTA–Fe^{II} (200 μM), 3% H_2O_2, the tested compounds (1–16 μM), and a phosphate buffer (67 mM, pH = 7.4) were contained in an assay mixture (4 mL). The assay mixtures were incubated at 37 °C for 30 min in a water bath. After this, the absorbance was measured at 555 nm. All the tests were run in triplicate and expressed as the mean. A_i was the absorbance in the presence of the tested compound; A_0 was the absorbance in the absence of tested compounds; A_c was the absorbance in the absence of tested compound, EDTA–Fe^{II}, H_2O_2. The suppression ratio (η_a) was calculated on the basis of $(A_i - A_0)/(A_c - A_0) \times 100\%$.

Acknowledgments

This work was supported by the National Natural Science Foundation of China (NSFC) (grant number 20871056), the Natural Science Foundation of Guangdong Province (grant number 8251063201000008), the Planned Item of Science and Technology of Guangdong Province (C1011220800060), the 211 Project Grant of Jinan University, and the Fundamental Research Funds for the Central Universities.

[1] C. M. Che, J. S. Huang, *Coord. Chem. Rev.* **2002**, *231*, 151–164.
[2] J. Liu, W. J. Zheng, S. Shi, C. P. Tan, J. C. Chen, K. C. Zheng, L. N. Ji, *J. Inorg. Biochem.* **2008**, *102*, 193–202.
[3] C. P. Tan, J. Liu, H. Li, W. J. Zheng, S. Shi, L. M. Chen, L. N. Ji, *J. Inorg. Biochem.* **2008**, *102*, 347–358.
[4] J. M. Rademaker-Lakhai, B. D. van, D. Pluim, J. H. Beijnen, J. H. Schellens, *Clin. Cancer Res.* **2004**, *10*, 3717–3727.
[5] C. G. Hartinger, S. Zorbas-Seifried, M. A. Jakupec, B. Kynast, H. Zorbas, B. K. Keppler, *J. Inorg. Biochem.* **2006**, *100*, 891–904.
[6] C. G. Hartinger, M. A. Jakupec, S. Zorbas-Seifried, M. Groessl, A. Egger, W. Berger, H. Zorbas, P. J. Dyson, B. K. Keppler, *Chem. Biodiversity* **2008**, *5*, 2140–2155.
[7] P. C. Bruijnincx, P. J. Sadler, *Curr. Opin. Chem. Biol.* **2008**, *12*, 197–206.
[8] M. A. Jakupec, M. Galanski, V. B. Arion, C. G. Hartinger, B. K. Keppler, *Dalton Trans.* **2008**, 183–194.
[9] P. J. Dyson, G. Sava, *Dalton Trans.* **2006**, 1929–1933.
[10] C. S. Allardyce, P. J. Dyson, *J. Cluster Sci.* **2001**, *12*, 563–569.
[11] F. Piccioli, S. Sabatini, L. Messori, P. Orioli, C. G. Hartinger, B. K. Keppler, *J. Inorg. Biochem.* **2004**, *98*, 1135–1142.
[12] O. Zava, S. M. Zakeeruddin, C. Danelon, H. Vogel, M. Gratzel, P. J. Dyson, *Chembiochem* **2009**, *10*, 1796–1800.
[13] F. Linares, M. A. Galindo, S. Galli, M. A. Romero, J. A. Navarro, E. Barea, *Inorg. Chem.* **2009**, *48*, 7413–7420.
[14] L. Bratsos, S. Jedner, T. Gianferrara, E. Alessio, *Chimia* **2007**, *61*, 692–697.
[15] X. J. Meng, M. L. Leyva, M. Jenny, I. Gross, S. Benosman, B. Fricker, S. Harlepp, P. Hebraud, A. Boos, P. Wlosik, *Cancer Res.* **2009**, *69*, 5458–5466.
[16] a) F. Schmitt, P. Govindaswamy, G. Süss-Fink, W. H. Ang, P. J. Dyson, L. J. Jeanneret, B. Therrien, *J. Med. Chem.* **2008**, *51*,1811–1816; b) H. E. Toma, K. Araki, *Coord. Chem. Rev.* **2000**, *196*, 307–329.
[17] Y. N. Liu, T. F. Chen, Y. S. Wong, W. J. Mei, X. M. Huang, F. Yang, J. Liu, W. J. Zheng, *Chemico-Biol. Interactions* **2010**, *183*, 349–356.
[18] T. M. Del, R. Gargallo, R. Eritja, J. Jaumot, *Anal. Biochem.* **2008**, *379*, 8–15.
[19] J. E. Klaunig, Y. Xu, J. S. Isenberg, S. Bachowski, K. L. Kolaja, J. Z. Jiang, D. E. Stevenson, E. F. Walborg Jr., *Environ. Health Perspect. Suppl.* **1998**, *106*, 289–295.
[20] T. F. Chen, Y. N. Liu, W. J. Zheng, J. Liu, Y. S. Wong, *Inorg. Chem.* **2010**, *49*, 6366–6368.
[21] a) Y. J. Liu, C. H. Zeng, Z. H. Liang, J. H. Yao, H. L. Huang, Z. Z. Li, F. H. Wu, *Eur. J. Med. Chem.* **2010**, *45*, 3087–3095; b) Y. J. Liu, Z. H. Liang, Z. Z. Li, C. H. Zeng, J. H. Yao, H. L. Huang, F. H. Wu, *BioMetals* **2010**, *23*, 739–752; c) M. Krstić, S. P. Sovilj, S. Grgurić-Šipka, I. R. Evans, S. Borozan, J. F. Santibanez, J. Kocić, *Eur. J. Med. Chem.* **2010**, *45*, 3669–3676.
[22] S. Shi, J. Liu, T. M. Yao, X. T. Geng, L. F. Jiang, Q. Y. Yang, L. Cheng, L. N. Ji, *Inorg. Chem.* **2008**, *47*, 2910–2912.
[23] T. F. Chen, Y. S. Wong, *J. Agric. Food Chem.* **2008**, *56*, 10574–10581.
[24] H. Pelicano, D. Carney, P. Huang, *Drug Resist. Updates* **2004**, *7*, 97–110.
[25] T. F. Chen, Y. S. Wong, *J. Agric. Food Chem.* **2008**, *56*, 4352–4358.

[26] D. F. Shi, R. T. Wheelhouse, D. Sun, L. H. Hurley, *J. Med. Chem.* **2001**, *44*, 4509–4523.
[27] B. P. Sullivan, D. J. Salmon, T. J. Meyer, *Inorg. Chem.* **1978**, *17*, 3334–3341.
[28] T. Mosman, *J. Immunol. Methods* **1983**, *65*, 55–63.
[29] M. C. Alley, D. A. Scudiero, A. Monks, M. L. Hursey, M. J. Czerwinski, D. L. Fine, B. J. Abbott, J. G. Mayo, R. H. Shoemaker, M. R. Boyd, *Cancer Res.* **1988**, *48*, 589–601.
[30] D. Griffith, S. Ceeco, E. Zangrando, A. Bergamo, G. Sava, C. J. Marmion, *J. Biol. Inorg. Chem.* **2008**, *13*, 511–520.
[31] S. L. Hempel, G. R. Buettner, Y. Q. O'Malley, D. A. Wessels, D. M. Flaherty, *Free Radical Biol. Med.* **1999**, *27*, 146–159.
[32] T. R. Li, Z. Y. Yang, B. D. Wang, D. D. Qin, *Eur. J. Med. Chem.* **2008**, *43*, 1688–1695.

Received: September 10, 2010
Published Online: March 16, 2011

